**Rapid Communications**

# Spectral correlations in Anderson insulating wires

M. Marinho and T. Micklitz
*Centro Brasileiro de Pesquisas Físicas, Rua Xavier Sigaud 150, 22290-180, Rio de Janeiro, Brazil*

(Received 6 November 2017; published 11 January 2018)

We calculate the spectral level-level correlation function of Anderson insulating wires for all three Wigner-Dyson classes. A measurement of its Fourier transform, the spectral form factor, is within reach of state-of-the-art cold atom quantum quench experiments, and we find good agreement with recent numerical simulations of the latter. Our derivation builds on a representation of the level-level correlation function in terms of a local generating function which may prove useful in other contexts.

DOI: 10.1103/PhysRevB.97.041406

*Introduction.* Localization due to quantum interference in disordered systems [1] is one of the cornerstones of condensed matter physics, with exciting recent developments such as topological Anderson insulators [2–6] and many-body localization [7,8]. Notwithstanding our profound understanding of the single-particle localization problem, examples of dynamical correlation functions within the Anderson insulating phase, which are accessible to direct experimental verification, are rare. The experimental challenge is to provide setups which allow for the controlled observation of strong localization via some tunable parameter [9]. On the theoretical side, one faces the notorious difficulty that Anderson insulators reside in the nonperturbative strong-coupling limit of a nonlinear field theory [10].

A series of recent papers proposes the direct observation of spectral correlations in Anderson insulators within a cold atom quantum quench experiment [11–14]. A specifically promising variant of this proposal builds on a cold atom realization of the kicked rotor and is within reach of state-of-the-art experiments [15]. The quench protocol is summarized as follows: (i) A cloud of cold atoms is prepared in an initial state with a well-defined momentum $\mathbf{k}_\mathrm{i}$, (ii) it is allowed to propagate freely under the influence of a disorder potential for some time $t$, at which (iii) the disorder is turned off and the atomic momentum distribution $\rho(\mathbf{k}_\mathrm{f},t)$ is measured. A forward-scattering peak at $\mathbf{k}_\mathrm{f} \simeq \mathbf{k}_\mathrm{i}$ is predicted to appear as a manifestation of an accumulation of those quantum coherence processes leading to strong Anderson localization. Within the quench setup, "time" plays the role of the control parameter and the genesis of the forward-scattering peak is described by the spectral form factor. The latter is the Fourier transform of the connected level-level correlation function,

$$K(\omega,L) = \nu_0^{-2}\left\langle \nu\left(\epsilon + \frac{\omega}{2}\right)\nu\left(\epsilon - \frac{\omega}{2}\right)\right\rangle_\mathrm{c}, \qquad (1)$$

where $\nu_0$ is the density of states (per spin) at the energy shell.

The theoretical study of level-level correlations (1) in disordered systems has a long history [16–25]. Analytical results are, however, only known in specific limits. In low-dimensional systems ($d < 3$), Eq. (1) describes how Wigner-Dyson statistics at small system sizes $L$ evolves into Poisson statistics with increasing size. The former is associated with nonintegrable chaotic dynamics, while the latter signals the breaking of ergodicity due to quantum localization [26,27]. Fully uncorrelated Poisson statistics only realizes in the thermodynamic limit of unbounded system sizes, and spectral correlations remain in finite size systems. It is these correlations which are accessible in the cold atom quench experiment, however, only asymptotic results are known for the experimentally relevant orthogonal and the symplectic symmetry class.

In this Rapid Communication, we derive the spectral level-level correlation function for Anderson insulating wires belonging to the three Wigner-Dyson classes. We show that the latter is readily calculated from the ground-state wave function of the transfer-matrix Hamiltonian for the supersymmetric $\sigma$ model reported in Ref. [28]. Our results are in perfect agreement with recent numerical simulations of the quench experiment [15], and their experimental verification would mark an important benchmark for our understanding of strong Anderson localization.

*Field theory.* We start out from the field theory description of the level-level correlation function for a $d$-dimensional disordered system [10,18,29],

$$K(\omega) = \frac{1}{64}\mathrm{Re}\left\langle\left[\int (dx)\mathrm{str}(k\Lambda Q_\Lambda)\right]^2\right\rangle_S. \qquad (2)$$

Here, the average, $\langle\cdots\rangle_S \equiv \int \mathcal{D}Q(\cdots)\exp(S)$, is with respect to the diffusive nonlinear $\sigma$-model action,

$$S = -\frac{\pi\tilde{\nu}_0}{8}\int (dx)\mathrm{str}[D(\partial_\mathbf{x} Q)^2 + 2i\omega\Lambda Q], \qquad (3)$$

where $D$ the classical diffusion constant, "str" the generalization of the matrix trace to "superspace," and $\int(dx) = 1$. The system belongs to one of the three Wigner-Dyson symmetry classes, characterized by the absence of time-reversal symmetry, $\mathcal{T} = 0$ (unitary class), presence of time-reversal and spin-rotational symmetry, $\mathcal{T}^2 = 1$ (orthogonal class), or presence of time-reversal and absence of spin-rotational symmetry, $\mathcal{T}^2 = -1$ (symplectic class). Throughout this Rapid Communication, we adopt the notation of Ref. [10] where $\tilde{\nu}_0 = \nu_0$ in the unitary and orthogonal, and $\tilde{\nu}_0 = 2\nu_0$ in the symplectic class. $Q$ is a supermatrix acting on an eight-dimensional graded space, which is the product of two-dimensional subspaces, referred to as "bosonic-fermionic" (bf), "retarded-advanced" (ra), and "time-reversal" (tr) sectors. Matrices $k \equiv \sigma_3^{\rm bf}$, $\Lambda \equiv \sigma_3^{\rm ra}$ break symmetry in bosonic-fermionic and advanced-retarded sectors, respectively. $\Lambda$ describes the classical, diffusive fixed point and $Q_\Lambda \equiv Q - \Lambda$ deviations from the latter. Drawing on the similarity of action (3) to Ginzburg-Landau theories for phase transitions, $\mathrm{str}(\Lambda Q)$ corresponds to a symmetry-breaking term relevant at large level separations or short time scales $t \sim \omega^{-1} \ll \Delta_\xi^{-1} \equiv \xi^2/D$, with $\xi$ the localization length. In this diffusive limit, $Q \simeq \Lambda$, which allows for a controlled perturbative expansion in Goldstone modes, viz., the diffusion modes of the disordered single-particle system. Strong Anderson localization sets in at $t \sim \omega^{-1} \sim \Delta_\xi^{-1}$ when large fluctuations restore the symmetry in the ra sector. This requires integration over the entire $Q$-field manifold and calls for nonperturbative methods. Such methods are available for quasi-one-dimensional geometries $L \gg L_\perp$, where the functional integral with action (3) takes the form of a path integral of a quantum mechanical particle with coordinate $Q$ and mass $\sim 1/D$, moving in a potential $\sim \mathrm{str}(\Lambda Q)$. The latter can be mapped onto the corresponding Schrödinger problem, and next we follow this strategy.

*Anderson insulating wires.* Concentrating then on a quasi-one-dimensional geometry, one needs to express the spectral correlation function Eq. (2) in terms of eigenfunctions of the Hamiltonian for the Schrödinger problem, known as the transfer-matrix Hamiltonian. This has been done in previous work [10,30]. The resulting equations for the relevant functions are, however, rather complex and closed solutions for all Wigner-Dyson classes are unknown. We therefore follow here a different route, which employs the graded symmetry of action (3) in order to derive Eq. (1) from a local generating function. The latter depends only on the ground-state wave function, i.e., "zero modes" of the transfer-matrix Hamiltonian. This implies a significant simplification of the problem, and allows for an exact calculation of correlations (1). We momentarily postpone the discussion of the rather technical derivation, and state the final expression for the generating function in the case of Anderson insulating wires $L \gg \xi \equiv \pi \tilde{\nu}_0 D/L$ [31],

$$K(\omega) = \frac{\xi}{2\beta L} \mathrm{Re} \int (dx) \partial_\eta \mathcal{F}(\eta,x) \Big|_{\eta=-\frac{i\omega}{\Delta_\xi}},$$
$$\mathcal{F}(\eta) = \frac{1}{2} \int dQ_0 \, \mathrm{str}(\Lambda Q_0) Y_0^2(Q_0). \tag{4}$$

Here, $Y_0$ is the ground-state wave function of the Schrödinger problem detailed below, and we introduced the symmetry parameter $\beta = 1(2)$ in the orthogonal and symplectic (unitary) class. Notice that in Eq. (4) we already integrated out some $c$ number and all Grassmann variables. That is, $Q_0$ here depends only on $c$-number variables from the compact interval $-1 \leqslant \lambda_{\rm f} \leqslant 1$ ("fermionic radial variables"), and noncompact interval $1 \leqslant \lambda_{\rm b}$ ("bosonic radial variables"). The precise number of radial variables depends on the symmetry class, i.e., $Q_0(\mathcal{R})$, with $\mathcal{R} = \{\lambda_{\rm f},\lambda_{\rm b}\}$, $\{\lambda_{\rm f},\lambda_{\rm b,1},\lambda_{\rm b,2}\}$, and $\{\lambda_{\rm f,1},\lambda_{\rm f,2},\lambda_{\rm b}\}$, in the unitary, orthogonal, and symplectic classes, respectively. Similarly, $dQ_0 = d\mathcal{R}\sqrt{g(\Lambda)}$, with Jacobians $\sqrt{g} = 1/(\lambda_{\rm b} - \lambda_{\rm f})^2$, $\sqrt{g} = (1-\lambda_{\rm f}^2)/(\lambda_1^2+\lambda_2^2+\lambda_{\rm f}^2-2\lambda_1\lambda_2\lambda_{\rm f}-1)^2$, and $\sqrt{g} = (\lambda_{\rm b}^2-1)/(\lambda_1^2+\lambda_2^2+\lambda_{\rm b}^2-2\lambda_1\lambda_2\lambda_{\rm b}-1)^2$ for the three symmetry classes, and $d\mathcal{R}$ the flat measure. For notational convenience, we suppress the graded index b,f in favor of the tr index 1,2. The ground-state wave function is a solution to the homogeneous equation,

$$\left[ -\Delta_Q + \frac{\eta}{2} \mathrm{str}(\Lambda Q_0) \right] Y_0(Q_0) = 0, \tag{5}$$

obeying the boundary condition $Y_0(\Lambda) = 1$, and we recall that at $Q_0 = \Lambda$ all radial coordinates $\lambda = 1$. Here, we introduced $\eta = -i\omega/\Delta_\xi$, and $\Delta_Q = \frac{1}{\sqrt{g}} \partial_\lambda \sqrt{g} g^{\lambda\rho} \partial_\rho$ is the Beltrami-Laplace operator on the $Q_0$-field manifold with repeated indices running over radial variables $\lambda,\rho \in \mathcal{R}$ and the metric tensor $g^{\lambda\rho} = |\lambda^2 - 1| \delta^{\lambda\rho}$ in all symmetry classes, with $\delta^{\lambda\rho}$ the Kronecker delta.

*Correlations from zero mode.* We may then use the Schrödinger equation to express $\mathrm{str}(\Lambda Q_0)\, Y_0 = -[2\Delta_Q + \eta\, \mathrm{str}(\Lambda Q_0)] Y_0'$ and $\eta\, \mathrm{str}(\Lambda Q_0)\, Y_0 = -2\Delta_Q Y_0$, and arrive at

$$\mathcal{F}(\eta) = \int dQ_0 (Y_0' \Delta_Q Y_0 - Y_0 \Delta_Q Y_0'), \tag{6}$$

where we introduced $Y_0' \equiv \partial_\eta Y_0$. Upon partial integration, this results in the boundary contribution

$$\mathcal{F}(\eta) = \int d\mathcal{R}\, \partial_\lambda \sqrt{g} g^{\lambda\rho} (Y_0' \partial_\rho Y_0 - Y_0 \partial_\rho Y_0'). \tag{7}$$

At this point we notice that the metric elements $g^{\lambda\rho}$ vanish at any boundary point $\lambda = 1$. At the same time, the Jacobian is singular at $Q_0 = \Lambda$ where all $\lambda_{\rm b},\lambda_{\rm f} = 1$. To deal with this situation we regularize the integral Eq. (7) in any of the variables $\lambda$, shifting the bound of integration to $1^\pm \equiv 1 \pm \epsilon$ with $\pm$ for a bosonic/fermionic variable. In the limit $\epsilon \searrow 0$, the boundary contribution $(\sqrt{g} g^{\lambda\rho})|_{\lambda=1^\pm}$ then reduces (up to a numerical factor) to a $\delta$ function in the remaining radial coordinates, fixing $Q_0 = \Lambda$. Noting further that $Y_0(\Lambda) = 1$ and $Y_0'(\Lambda) = 0$, we arrive at the remarkably simple expression

$$\mathcal{F}(\eta) = -2\partial_{\lambda_{\rm f}} Y_0' |_{Q=\Lambda}, \tag{8}$$

where in the symplectic class $\lambda_{\rm f}$ can be either $\lambda_{1,2}$. It can be verified that $\partial_\lambda Y_0'|_{Q=\Lambda} = \pm \partial_\rho Y_0'|_{Q=\Lambda}$, where the positive sign applies if $\lambda$ and $\rho$ are both bosonic or fermionic radial variables and the negative sign else. This guarantees that Eq. (8) does not depend on the regularization scheme, and one may, e.g., symmetrize the result in the radial variables [32]. An equivalent relation between the ground-state wave function and the generating function for spectral correlations has been previously encountered for the unitary class [33,34]. In this case the derivation is built upon a mapping of the localization problem in the unitary class to the three-dimensional Coulomb problem [35]. The above Eq. (8) shows that the simple relation is not accidental but applies to all Wigner-Dyson symmetry classes.

Using then the recent results of Refs. [28,32] for the ground-state wave functions, we find ($z_\eta \equiv 4\sqrt{\eta}$)

$$\mathcal{F}^{\rm U}(\eta) = -8 I_0(z_\eta) K_0(z_\eta), \tag{9}$$

$$\mathcal{F}^{\rm O}(\eta) = -4[I_0(z_\eta)K_0(z_\eta) + I_1(z_\eta)K_1(z_\eta)], \tag{10}$$

$$\mathcal{F}^{\rm Sp}_\pm(\eta) = -4\{[I_0(z_\eta) \pm 1]K_0(z_\eta) + I_1(z_\eta)K_1(z_\eta)\}, \tag{11}$$

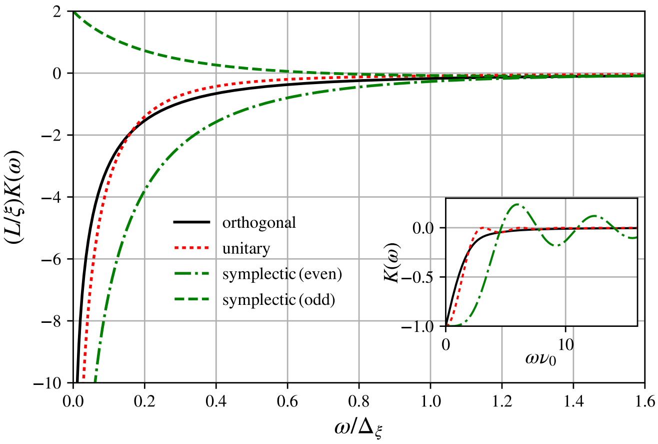


FIG. 1. Level-level correlations in Anderson insulating wires for the Wigner-Dyson classes. The residual level attraction in the symplectic class with an odd number of channels reflects the presence of a topologically protected metallic channel. The inset shows for comparison the Wigner-Dyson spectral correlations of fully chaotic systems.

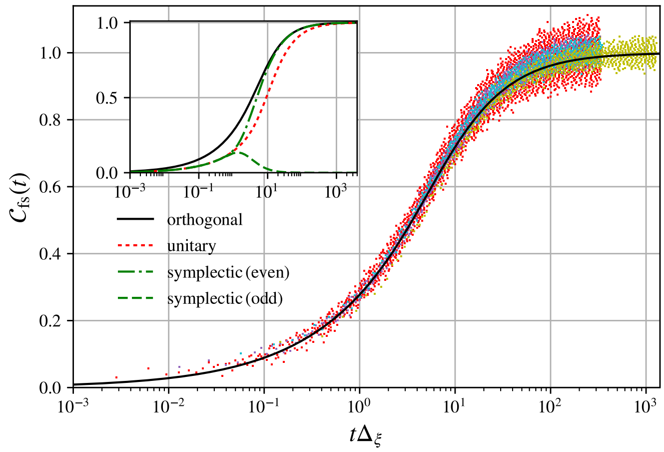


FIG. 2. Forward-scattering peak in the orthogonal class. Points are numerical data from a recent simulation of the quantum quench experiment in a kicked rotor setup [15]. Different colors correspond to different sets of system parameters, and the solid line shows Eq. (20) without any fitting parameter [43]. Insets: Forward-scattering peak for all Wigner-Dyson classes; see main text for a discussion.

where "U," "O," and "Sp" refers to the unitary, orthogonal, and symplectic symmetry class, respectively, and $+/-$ indicates an even/odd number of channels.

*Spectral correlations.* From Eqs. (9)–(11) we find the level-level correlations in Anderson insulating wires for all three Wigner-Dyson classes,

$$K(\omega) = \frac{32\xi}{\beta L}\mathrm{Re}\,\mathcal{K}(z_\eta)|_{z_\eta=4\sqrt{-i\omega/\Delta_\xi}}, \tag{12}$$

where

$$\mathcal{K}^{\mathrm{U}}(z_\eta) = [K_1(z_\eta)I_0(z_\eta) - K_0(z_\eta)I_1(z_\eta)]/z_\eta, \tag{13}$$

$$\mathcal{K}^{\mathrm{O}}(z_\eta) = K_1(z_\eta)I_1(z_\eta)/z_\eta^2, \tag{14}$$

$$\mathcal{K}^{\mathrm{Sp}}_\pm(z_\eta) = K_1(z_\eta)[I_1(z_\eta) \pm z_\eta/2]/z_\eta^2. \tag{15}$$

Equations (12)–(15) are the main result of this Rapid Communication. Strict Poisson statistics only applies for $\lim_{L\to\infty} K(L,\omega) = 0$, and correlations between localized eigenstates remain in any finite system. At large level separation ($s \equiv \omega/\Delta_\xi \gg 1$) these reflect the classically diffusive dynamics on short time scales, on which quantum interference processes remain largely undeveloped. Correlations of close-by levels ($s \equiv \omega/\Delta_\xi \lesssim 1$), on the other hand, store information on the long-time limit, i.e., the deep quantum regime in which the remaining dynamical processes are due to tunneling between almost degenerate, far-distant localized states [21,36,37]. The crossover between these two limits, described by Eqs. (12)–(15), is shown in Fig. 1. For a comparison with fully chaotic systems we also show in the inset the corresponding Wigner-Dyson correlations with their characteristic level repulsion at small level separations, and contrasting the residual logarithmic level repulsion between localized states.

From the above expression, one readily recovers asymptotic correlations of far-distant levels $s \gg 1$, applying to all Wigner-Dyson classes [38],

$$\frac{L}{\xi}K(s) = -\frac{1}{4\sqrt{2}\beta}\left(\frac{1}{s^{3/2}} - \frac{(-1)^\beta 3}{128 s^{5/2}} + \cdots\right), \tag{16}$$

with the leading Altshuler-Shklovskii contribution [19,39]. For small level separations and systems in the unitary, orthogonal, or symplectic class with an even number of channels ($s \ll 1$),

$$\frac{L}{\xi}K(s) = -a_\beta[\log(1/4s) - 2\gamma + b_\beta + c_\beta \pi s + \cdots], \tag{17}$$

where $\gamma \simeq 0.577$ the Euler-Mascheroni constant, $a_{\mathrm{U,Sp+}} = 8$, $a_{\mathrm{O}} = 4$, $b_{\mathrm{U}} = 0$, $b_{\mathrm{O}} = 1/2$, $b_{\mathrm{Sp+}} = 3/4$, and $c_{\mathrm{U}} = 3$, $c_{\mathrm{O}} = 2$, $c_{\mathrm{Sp+}} = 3/2$. In the symplectic class with an odd number of channels ($s \ll 1$),

$$\frac{L}{\xi}K_-^{\mathrm{Sp}}(s) = 2 - 4\pi s - [(8s)^2/3]\log(s) + \cdots, \tag{18}$$

which signals the presence of a single topologically protected metallic channel (see also Fig. 1).

*Forward peak.* The form factor derived from the above results describes the genesis of the forward-scattering peak in the quantum quench setup discussed in the Introduction [32,40],

$$\mathcal{C}^{\mathrm{U}}_{\mathrm{fs}}(t) = \theta(t)I_0(8/t\Delta_\xi)e^{-8/t\Delta_\xi}, \tag{19}$$

$$\mathcal{C}^{\mathrm{O}}_{\mathrm{fs}}(t) = \theta(t)[I_0(8/t\Delta_\xi) + I_1(8/t\Delta_\xi)]e^{-8/t\Delta_\xi}, \tag{20}$$

$$\mathcal{C}^{\mathrm{Sp},\pm}_{\mathrm{fs}}(t) = \tfrac{1}{2}\big[\mathcal{C}^{\mathrm{O}}_{\mathrm{fs}}(t) \pm \theta(t)e^{-4/t\Delta_\xi}\big]. \tag{21}$$

Here, we have normalized the peak with respect to its saturation value $\lim_{t\to\infty}\mathcal{C}_{\mathrm{fs}}(t)$. The forward peak in the unitary class has been calculated previously [14,41]. Corresponding results for the experimentally relevant orthogonal class [42] and the symplectic class have been unknown. Figure 2 displays a comparison of our results with recent numerical simulations of the quantum quench experiment in the orthogonal class [41].

The solid line is Eq. (20) and shows perfect agreement with the numerical data without using any fitting parameter. The forward peaks for all Wigner-Dyson classes are displayed in the inset of Fig. 2. $\mathcal{C}_{\rm fs}^{\rm O}$ is readily understood as a sum of diagrams involving only ladders ("diffuson modes") $\mathcal{C}_{\rm fs}^{\rm U}$, and diagrams containing crossed ladders ("Cooperon modes"). $\mathcal{C}_{\rm fs}^{\rm Sp,\pm}$ follows the signal of the unitary class at short times, $\tau \equiv t\Delta_\xi \ll 1$, staying a factor of 2 below the signal in the orthogonal class, and becomes sensitive to the channel number once $\tau \equiv t\Delta_\xi \gtrsim 0.1$. For an odd channel number the signal in the symplectic class then decays to zero as $\mathcal{C}_{\rm fs}^{\rm Sp,-} \sim 4/\tau^2 - 64/(3\tau^3) + \cdots$, indicating delocalization due to the presence of the topologically protected channel. Long- and short-time signals in the remaining cases can be summarized as ($\tau \equiv t\Delta_\xi$)

$$\mathcal{C}_{\rm fs}(\tau) = \begin{cases} a_\alpha \tau^{1/2} + b_\alpha \tau^{3/2} + \cdots, & s \ll 1, \\ 1 - c_\alpha/\tau + d_\alpha/\tau^2 + \cdots, & s \gg 1, \end{cases} \quad (22)$$

where $a_{\rm O} = 2a_{\rm U,Sp+} = 1/(2\sqrt{\pi})$, $b_{\rm O} = -2b_{\rm U} = 2b_{\rm Sp+} = -1/(128\sqrt{\pi})$, $c_{\rm O,Sp+} = c_{\rm U}/2 = 4$, and $d_{\rm O} = d_{\rm U}/3 = 4d_{\rm Sp_+}/3$.

*Local generating function.* The analysis above relied on the representation of the level-level correlation function in terms of a local generating function. The latter derives from the graded symmetry of action (3), which is evident in the polar parametrization $Q = UQ_0U^{-1}$ [10]. Here, matrices $U$ are diagonal in the ra sector and contain all anticommuting variables, while $Q_0 = \cos\hat\theta\sigma_3^{\rm ra} - \sin\hat\theta\sigma_2^{\rm ra}$ has an off-diagonal structure in the latter [32]. The block-diagonal matrices in the bf sector $\hat\theta = {\rm diag}(i\hat\theta_{\rm b},\hat\theta_{\rm f})_{\rm bf}$, with $\hat\theta_{\rm b,f}$ matrices in the tr sector, are conveniently parametrized by the noncompact and compact radial variables introduced earlier, $-1 \leqslant \lambda_{\rm f} \equiv \cos\theta_{\rm f} \leqslant 1, 1 \leqslant \lambda_{\rm b} \equiv \cosh\theta_{\rm b}$ [10]. The graded symmetry manifests itself in the invariance of action (3) under constant rotations $\bar U$ sharing the symmetries of $U$, $U \mapsto \bar U U$. This invariance can be used to linearly shift Grassmann variables in the preexponential correlation function, and, e.g., implies that finite contributions to the superintegral Eq. (2) may only derive from the maximal polynomial of Grassmann variables $P_{\mathcal{G}}$ [44]. It is then convenient to introduce (unnormalized) maximal polynomials of Grassmann variables in retarded/advanced sectors $P_{\mathcal{G}}^{\rm r/a}$ with $P_{\mathcal{G}} = P_{\mathcal{G}}^{\rm r}P_{\mathcal{G}}^{\rm a}$ and the generating function $\mathcal{F}(\eta,\mathbf{x}) \equiv \langle \frac{\{{\rm str}[k\Lambda Q_\Lambda(\mathbf{x})]\}^2}{{\rm str}[\Lambda Q(\mathbf{x})]}\rangle_S$. Notice that in the quantum-dot limit $Q$ becomes $\mathbf{x}$ independent, and the generation of Eq. (2) by $\partial_\eta\mathcal{F}$ is immediately evident. For general $d$-dimensional systems, on the other hand, a straightforward calculation shows that $\mathcal{F}(\eta,\mathbf{x}) = \langle {\rm str}(\cos\hat\theta_{\mathbf{x}})P_{\mathcal{G},\mathbf{x}}^{\rm r}\rangle_S$ [32,45], and similarly one finds

$$\partial_\eta\mathcal{F}(\eta,\mathbf{x}) \propto \int (dy)\langle \mathcal{C}_{\mathbf{x},\mathbf{y}}P_{\mathcal{G},\mathbf{x}}\rangle_S, \quad (23)$$

$$K(\omega) \propto \int (dx)\int (dy)\,\langle \mathcal{C}_{\mathbf{x},\mathbf{y}}P_{\mathcal{G},\mathbf{x}}^{\rm a}P_{\mathcal{G},\mathbf{y}}^{\rm r}\rangle_S, \quad (24)$$

with $\mathcal{C}_{\mathbf{x},\mathbf{y}} = {\rm str}(\cos\hat\theta_{\mathbf{x}}){\rm str}(\cos\hat\theta_{\mathbf{y}})$. The graded symmetry can now be used to shift $P_{\mathcal{G},\mathbf{x}(\mathbf{y})}^{\rm r} \mapsto P_{\mathcal{G},\mathbf{x}}^{\rm r} + P_{\mathcal{G},\mathbf{y}}^{\rm r}$, in the first (second) term, which implies that Eq. (2) is generated from the local correlation function for general $d$-dimensional systems. Indeed, keeping numerical factors, one finds $K(\omega) = -(16\pi\tilde\nu_0)^{-1}\,{\rm Im}\int (dx)\partial_\omega\mathcal{F}(\omega,\mathbf{x})$, and $\mathcal{F}(\eta) = \frac{8}{\beta}\langle {\rm str}(\cos\hat\theta_{\mathbf{x}})P_{\mathcal{G},\mathbf{x}}^0\rangle_S$ with $P_{\mathcal{G}}^0$ now the normalized maximal polynomial of Grassmann variables [32]. Upon integration over the latter, one arrives at Eq. (4) for the Anderson insulating wires. Notice that similar ideas have previously been applied in the context of the replicated $\sigma$ model [46] and parametric correlations [47]. The representation of level-level correlations in terms of the local generating function may also prove to be useful in other contexts [48].

*Summary.* We have shown that spectral correlations in the Wigner-Dyson classes can be calculated within the supersymmetric $\sigma$ model from a local generating function. In Anderson insulating wires this reveals a simple relation between level-level correlations and the ground-state wave function of the transfer-matrix Hamiltonian, which allowed us to derive spectral correlation functions for all Wigner-Dyson classes. The experimental observation of the spectral form factor is within reach of state-of-the-art cold atom quantum quench experiments, and a parameter-free comparison of our findings with recent numerical simulations of the latter shows perfect agreement. The experimental verification of the results reported here would mark an important benchmark for our understanding of strong Anderson localization.

*Acknowledgments.* We thank G. Lemarié for providing us with their simulation data of the quantum quench experiment. T.M. acknowledges financial support by Brazilian agencies CNPq and FAPERJ.

[1] P. W. Anderson, Phys. Rev. **109**, 1492 (1958).
[2] C. W. Groth, M. Wimmer, A. R. Akhmerov, J. Tworzydlo, and C. W. J. Beenakker, Phys. Rev. Lett. **103**, 196805 (2009).
[3] J. Li, R.-L. Chu, J. K. Jain, and S.-Q. Shen, Phys. Rev. Lett. **102**, 136806 (2009).
[4] W. DeGottardi, D. Sen, and S. Vishveshwara, Phys. Rev. Lett. **110**, 146404 (2013).
[5] I. Mondragon-Shem, T. L. Hughes, J. Song, and E. Prodan, Phys. Rev. Lett. **113**, 046802 (2014).
[6] A. Altland, D. Bagrets, and A. Kamenev, Phys. Rev. B **91**, 085429 (2015).
[7] D. Basko, I. Aleiner, and B. Altshuler, Ann. Phys. **321**, 1126 (2006).
[8] I. V. Gornyi, A. D. Mirlin, and D. G. Polyakov, Phys. Rev. Lett. **95**, 206603 (2005).
[9] J. Chabé, G. Lemarié, B. Grémaud, D. Delande, P. Szriftgiser, and J. C. Garreau, Phys. Rev. Lett. **101**, 255702 (2008); J. Billy *et al.*, Nature (London) **453**, 891 (2008); G. Roati *et al.*, *ibid.* **453**, 895 (2008).
[10] K. B. Efetov, *Supersymmetry in Disorder and Chaos* (Cambridge University Press, Cambridge, UK, 1999).
[11] T. Karpiuk, N. Cherroret, K. L. Lee, B. Grémaud, C. A. Müller, and C. Miniatura, Phys. Rev. Lett. **109**, 190601 (2012).
[12] K. L. Lee, B. Grémaud, and C. Miniatura, Phys. Rev. A **90**, 043605 (2014).

[13] S. Ghosh, N. Cherroret, B. Grémaud, C. Miniatura, and D. Delande, Rev. A **90**, 063602 (2014).

[14] T. Micklitz, C. A. Müller, and A. Altland, Phys. Rev. Lett. **112**, 110602 (2014).

[15] G. Lemarié, C. A. Müller, D. Guéry-Odelin, and C. Miniatura, Phys. Rev. A **95**, 043626 (2017).

[16] L. P. Gor'kov and G. M. Eliashberg, Zh. Eksp. Teor. Fiz. **48**, 1407 (1965) [Sov. Phys. JETP **21**, 940 (1965)].

[17] K. B. Efetov, Zh. Eksp. Teor. Fiz. **83**, 833 (1982).

[18] K. B. Efetov, Adv. Phys. **32**, 53 (1983).

[19] B. L. Altshuler and B. I. Shklovskii, Zh. Eksp. Teor. Fiz. **91**, 220 (1986) [Sov. Phys. JETP **64**, 127 (1986)].

[20] B. L. Altshuler, I. Kh. Zharekeshev, S. A. Kotochigova, and B. I. Shklovskii, Zh. Eksp. Teor. Fiz. **94**, 343 (1988) [Sov. Phys. JETP **67**, 625 (1988)].

[21] U. Sivan and Y. Imry, Phys. Rev. B **35**, 6074 (1987).

[22] I. Kh. Zharekeshev, Sov. Phys. Solid State **31**, 65 (1989).

[23] F. M. Izrailev, Phys. Rep. **196**, 299 (1990).

[24] B. I. Shklovskii, B. Shapiro, B. R. Sears, P. Lambrianides, and H. B. Shore, Phys. Rev. B **47**, 11487 (1993).

[25] S. N. Evangelou and E. N. Economou, Phys. Rev. Lett. **68**, 361 (1992).

[26] C. E. Porter, *Statistical Properties of Spectra: Fluctuations* (Academic, New York, 1965).

[27] F. Haake, *Quantum Signatures of Chaos* (Springer, Berlin, Heidelberg, 2010).

[28] E. Khalaf and P. M. Ostrovsky, Phys. Rev. B **96**, 201105(R) (2017).

[29] K. B. Efetov and A. Larkin, Sov. Phys. JETP **58**, 444 (1983).

[30] A. Altland and D. Fuchs, Phys. Rev. Lett. **74**, 4269 (1995).

[31] The localization length here is always that for the orthogonal class, i.e., $\xi_{\rm O} = \xi$, while $\xi_{\rm U} = 2\xi$ and $\xi_{\rm Sp} = 4\xi$.

[32] See Supplemental Material at http://link.aps.org/supplemental/10.1103/PhysRevB.97.041406, where we summarize polar coordinates and zero modes for the Wigner-Dyson classes, and present details on the local generating function and the calculation of the forward scattering peak.

[33] T. Micklitz, Phys. Rev. B **93**, 094201 (2016).

[34] Correcting a factor 4 in Ref. [33].

[35] M. A. Skvortsov and P. M. Ostrovsky, JETP Lett. **85**, 72 (2007).

[36] N. F. Mott, Philos. Mag. **22**, 7 (1970).

[37] See, e.g., D. A. Ivanov, M. A. Skvortsov, P. M. Ostrovsky, and Ya. V. Fominov, Phys. Rev. B **85**, 035109 (2012).

[38] I. S. Gradsteyn and I. M. Ryzhik, *Table of Integrals, Series, and Products* (Academic, New York, 2000).

[39] E. Akkermans and G. Montambaux, *Mesoscopic Physics of Electrons and Photons* (Cambridge University Press, Cambridge, UK, 2007).

[40] That is, up to a normalization factor $\mathcal{C}_{\rm fs}(t) = \int_{-\infty}^{\infty} d\omega e^{-i\omega t}\partial_\eta \mathcal{F}(\eta)$.

[41] Notice that here we use $\Delta_\xi \equiv \Delta_\xi^{\rm O} = D/\xi_{\rm O}^2$ with $\xi_{\rm O}$ the localization length in the orthogonal class, and, e.g., $\Delta_\xi^{\rm U} = \Delta_\xi^{\rm O}/4$; see also Ref. [31].

[42] F. Jendrzejewski, K. Müller, J. Richard, A. Date, T. Plisson, P. Bouyer, A. Aspect, and V. Josse, Phys. Rev. Lett. **109**, 195302 (2012).

[43] The universal curve is obtained after accounting for finite Ehrenfest times and with Heisenberg times $\sim 1/\Delta_\xi$ independently determined from the wave-packet dynamics (see Ref. [15] for further details).

[44] M. Zirnbauer, Nucl. Phys. B **265**, 375 (1985).

[45] The pure $c$-number boundary term here vanishes.

[46] R. A. Smith, I. V. Lerner, and B. L. Altshuler, Phys. Rev. B **58**, 10343 (1998).

[47] N. Taniguchi, B. D. Simons, and B. L. Altshuler, Phys. Rev. B **53**, R7618(R) (1996).

[48] K. S. Tikhonov and A. D. Mirlin, Phys. Rev. B **94**, 184203 (2016).